

Paleoceanographic response of monsoonal variations in the northwestern Arabian Sea during Late Quaternary: Faunal and sedimentologic record

Ajai K. Rai and S. S. Das

Department of Earth and Planetary Sciences
Nehru Science Centre, University of Allahabad
Allahabad 211002, INDIA

*E-mail: raikajai@gmail.com

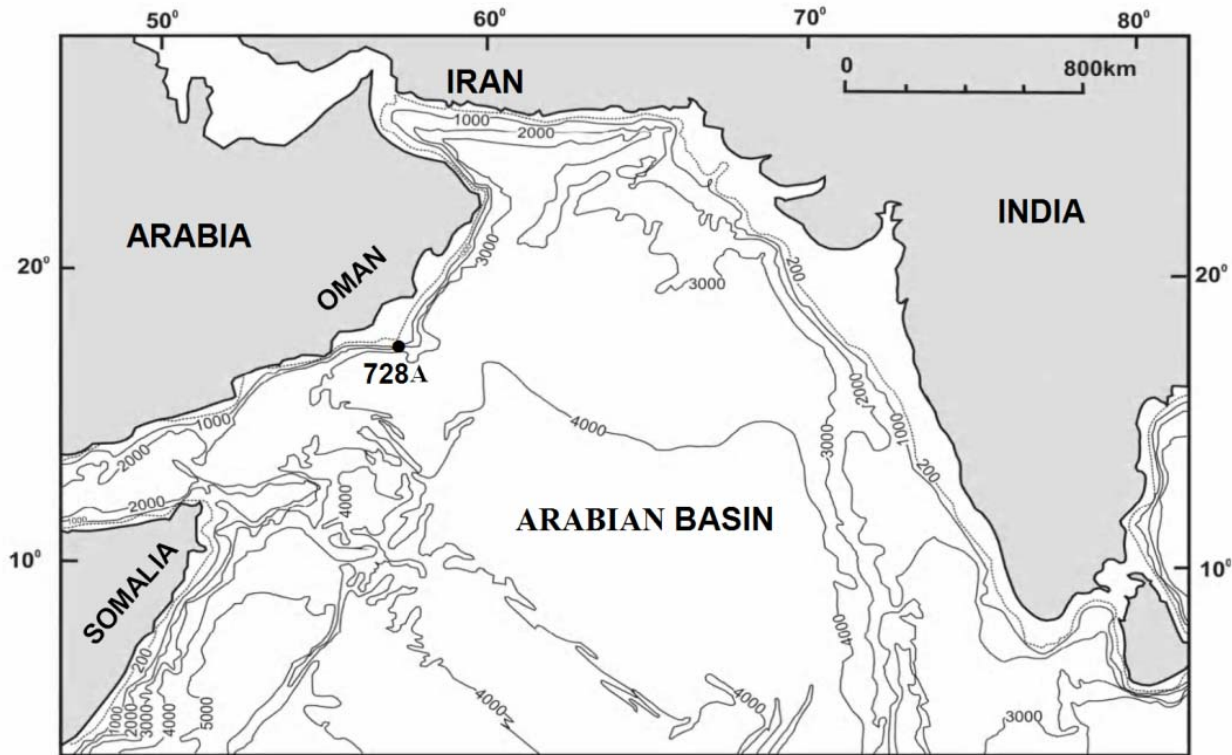
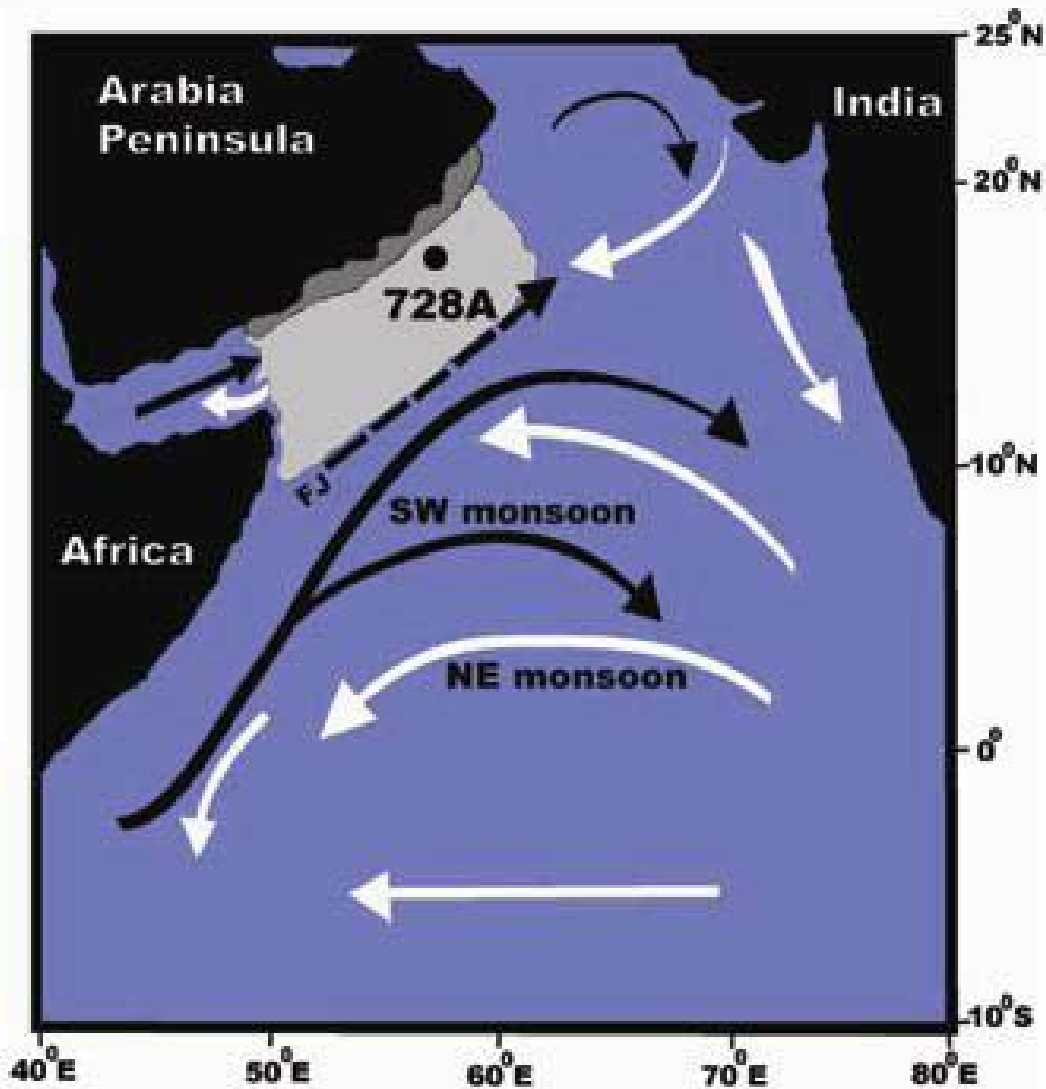


Figure 1

Location map and bathymetric profile of ODP site 728 A .
(Redrawn after Debrant, et al., 1991)

Water depth: **1428m**, Core length : **22.0m**

Latitude : **17°40.790' N** , Longitude : **57°49.553' E**



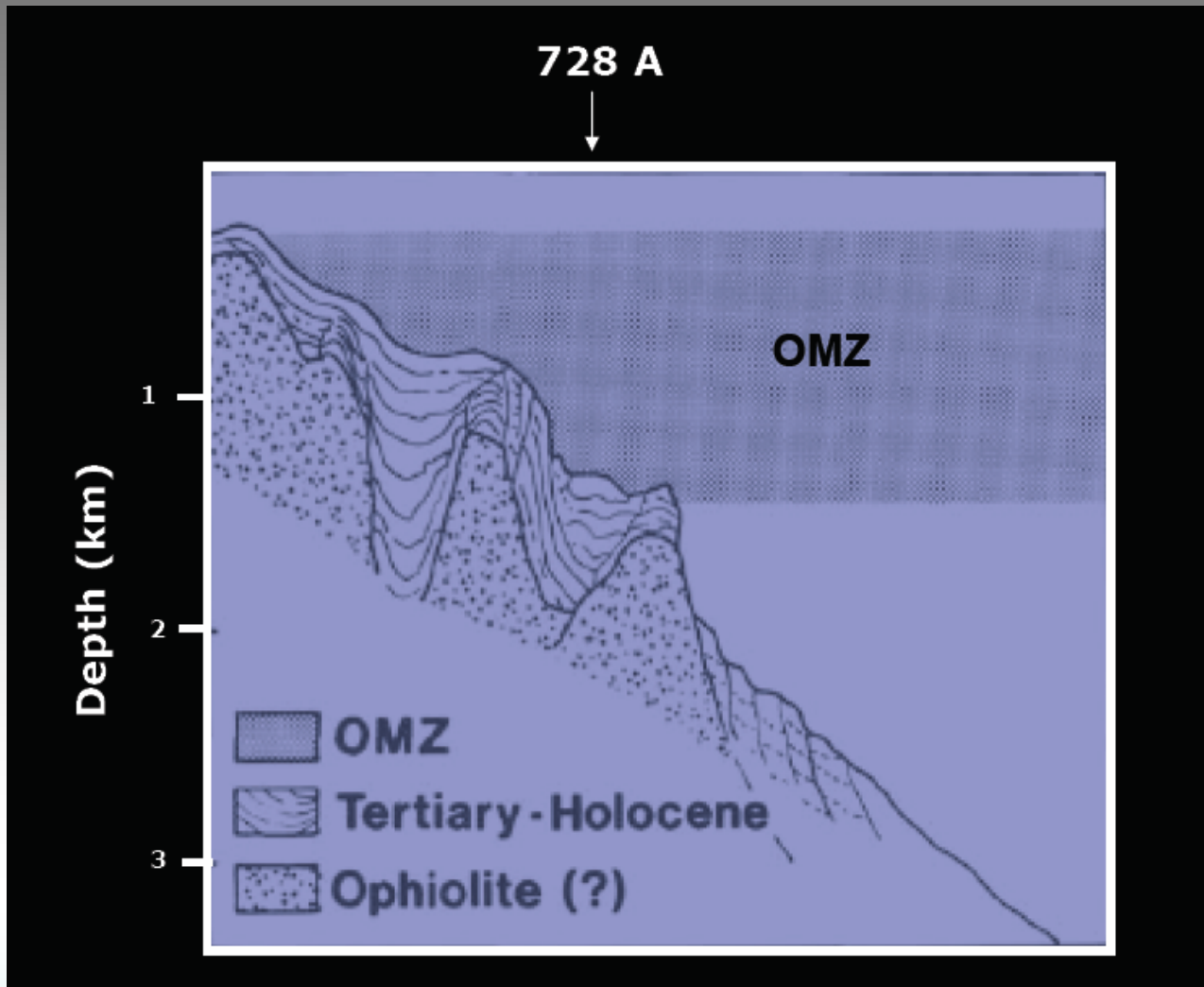
Surface hydrography in the Arabian Sea. A strong clockwise surface ocean circulation (black arrows) develops during the SW summer monsoon, which follows the direction of the Findlater Jet (FJ, arrows with broken line). Coastal upwelling area is indicated by dark grey; and the open ocean upwelling area by light grey. Anticlockwise NE winter monsoonal circulation is indicated by white arrows.

SW summer monsoon

: Coastal & open-ocean upwelling

NE winter monsoon

: Sea surface cooling & convective overturning

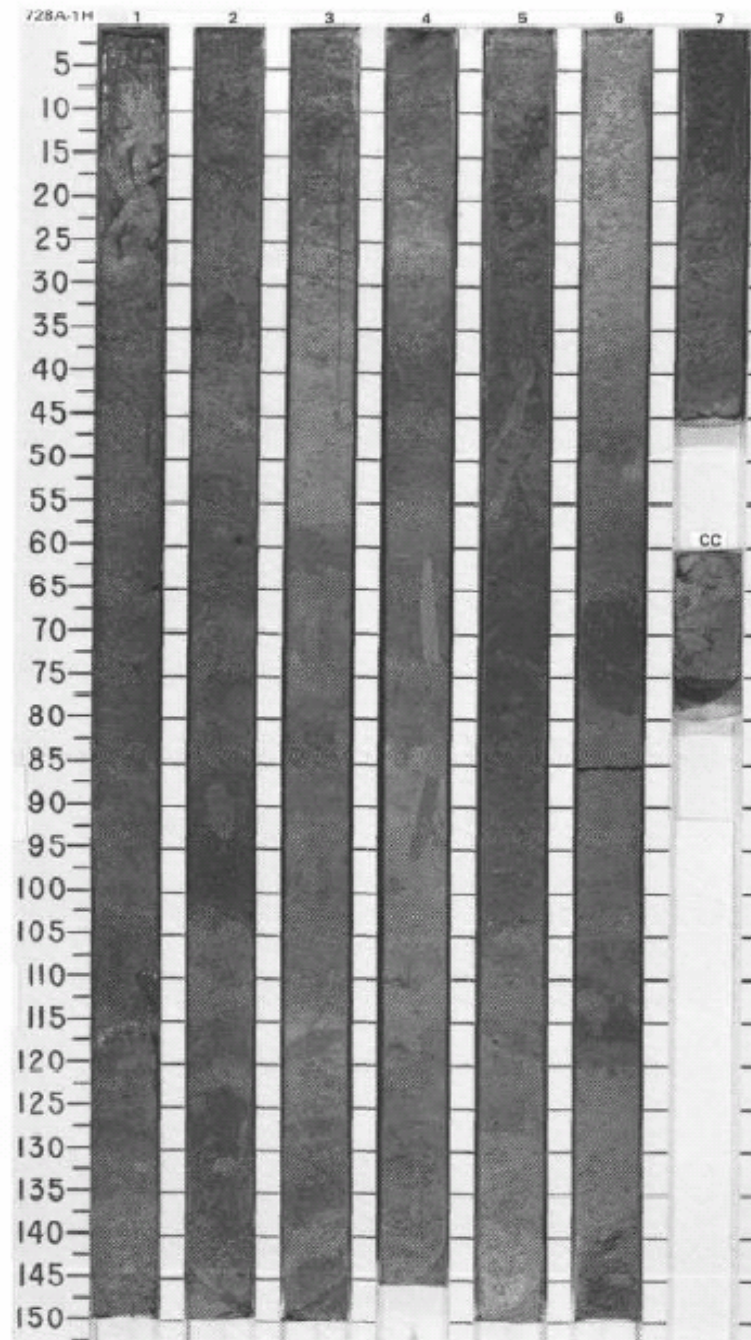
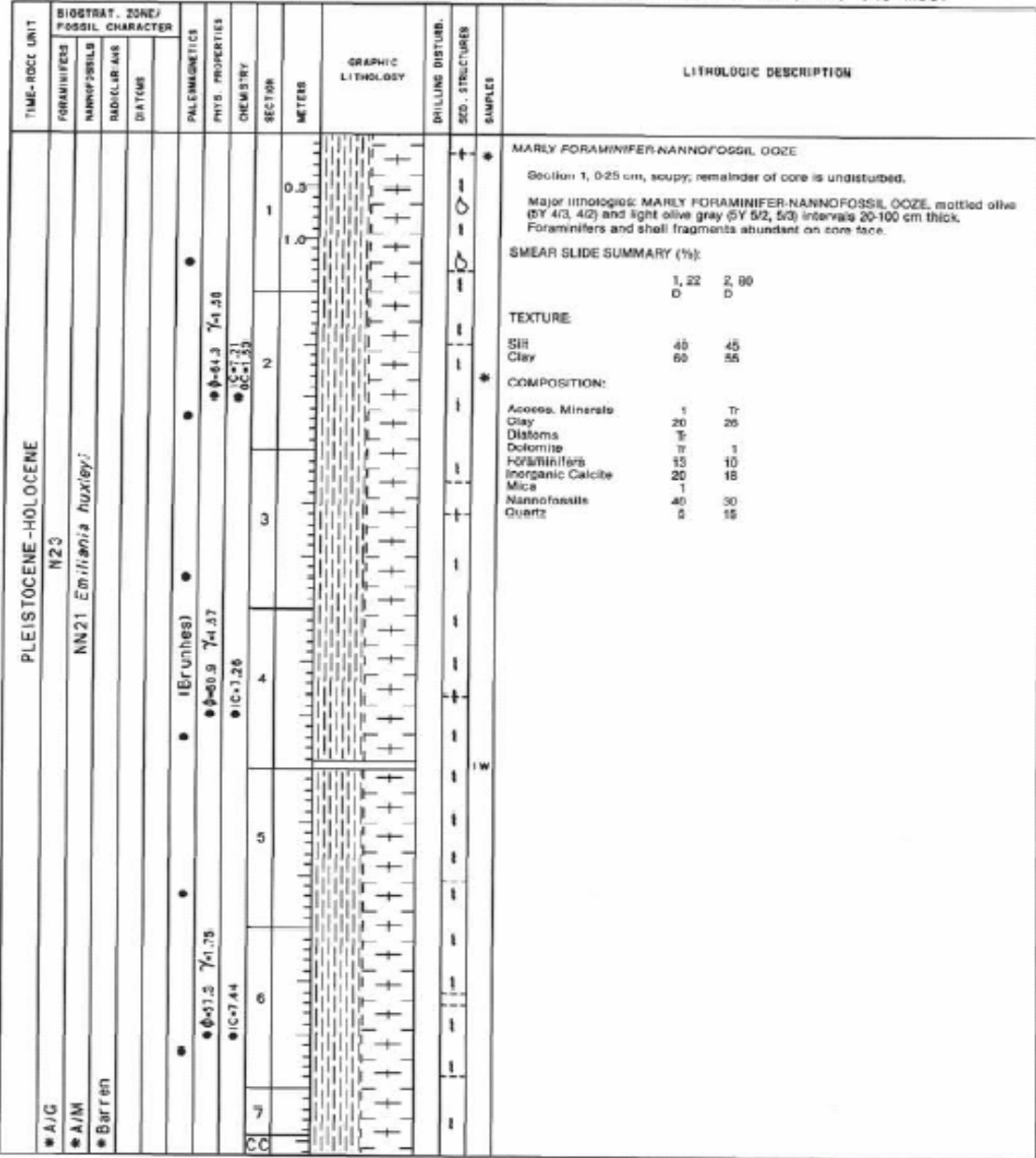


Schematic profile showing the structure of the Oman margin and the oxygen minimum zone (OMZ). Site 728A is located at the lower limit of OMZ.

Selection of this site is due to ;

Suitability to understand the complicated pattern of past upwelling and surface productivity in response to both SW & NE monsoonal variations.

Location of this site at the lower limit of the OMZ is suitable to record the influence of changes in intensity and vertical distribution of OMZ.



Materials and Methods

Total number of core samples : 90

Quantity of each sample : Apporx. 10 cm³

**Dominant Lithology : Foraminifera-rich
nannofossil ooze**

Sample processing by Wet Sieving Method : Foraminiferal study

Size fraction studied : Over 125 μm

Picking and mounting of about 300 planktic foraminiferal tests from each sample.

Bulk Sediment : Biogenic carbonate, organic matter & terrigenous matter

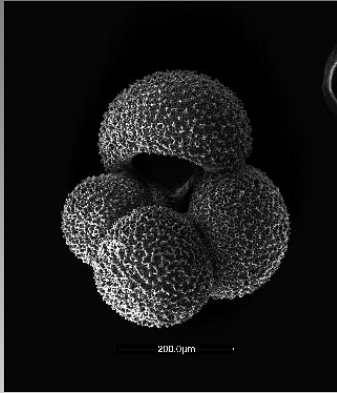
Paleoceanographic Parameters

Relative abundance of planktic foraminifera : **Upwelling & productivity record**

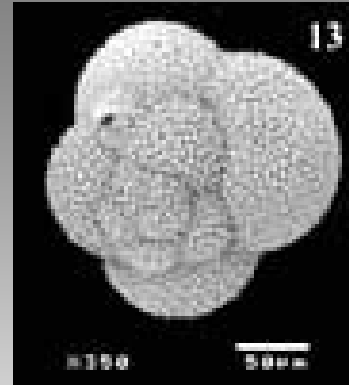
Pteropod accumulation & foraminiferal fragmentation : **OMZ & dissolution Record**

Organic Matter & Biogenic Carbonate : **Productivity record**

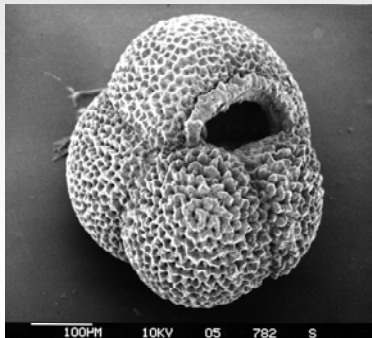
Dominant Planktic Foraminiferal Species



Globigerina bulloides
(coastal upwelling species)



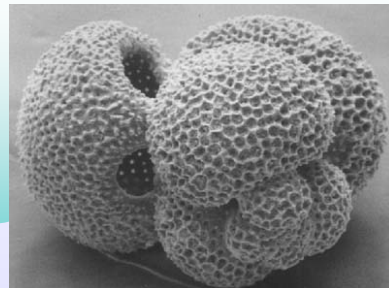
Globigerinita glutinata
(open-ocean upwelling species)



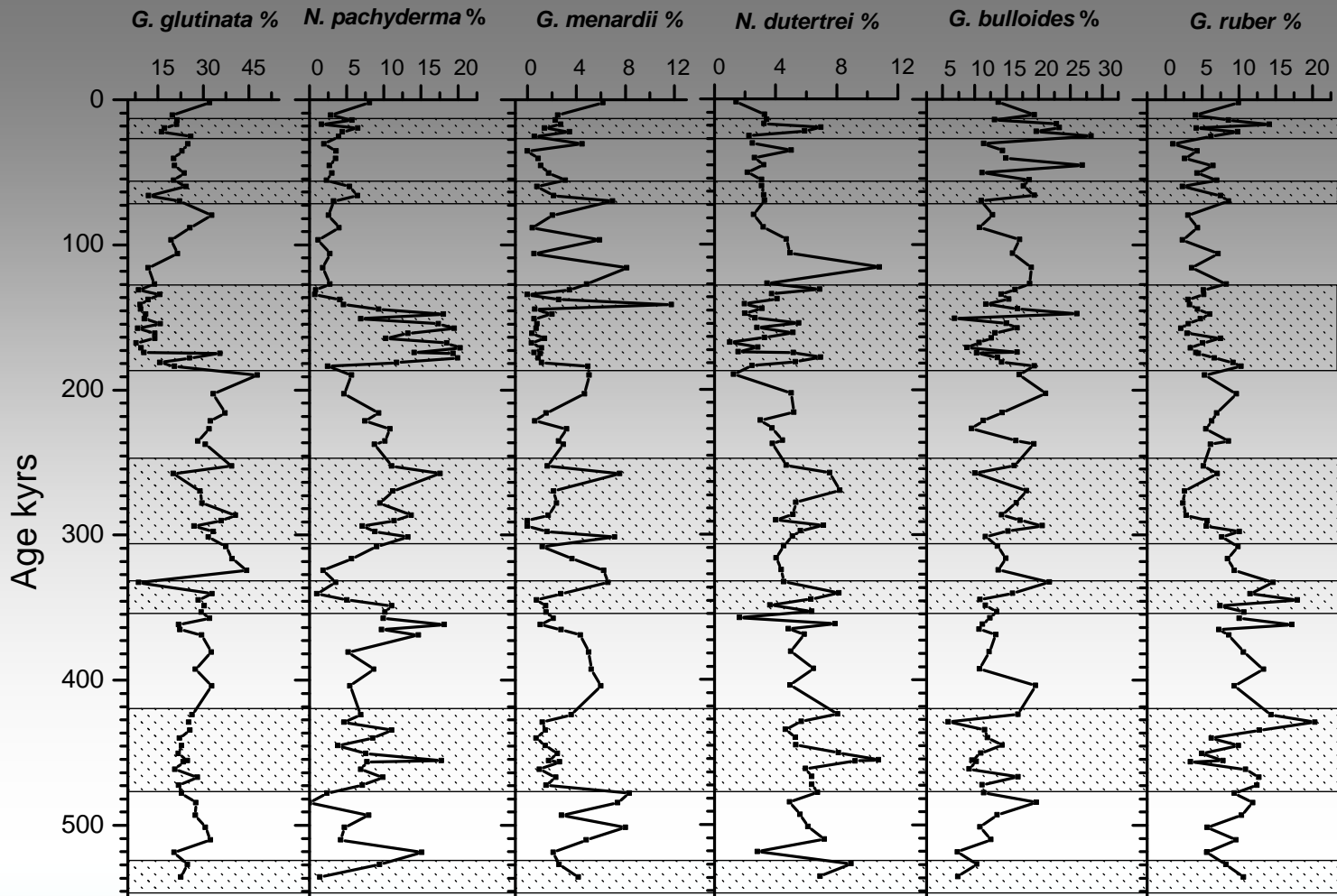
Neogloboquadrina pachyderma
(subpolar to polar species in more stratified, deep mixed layer)



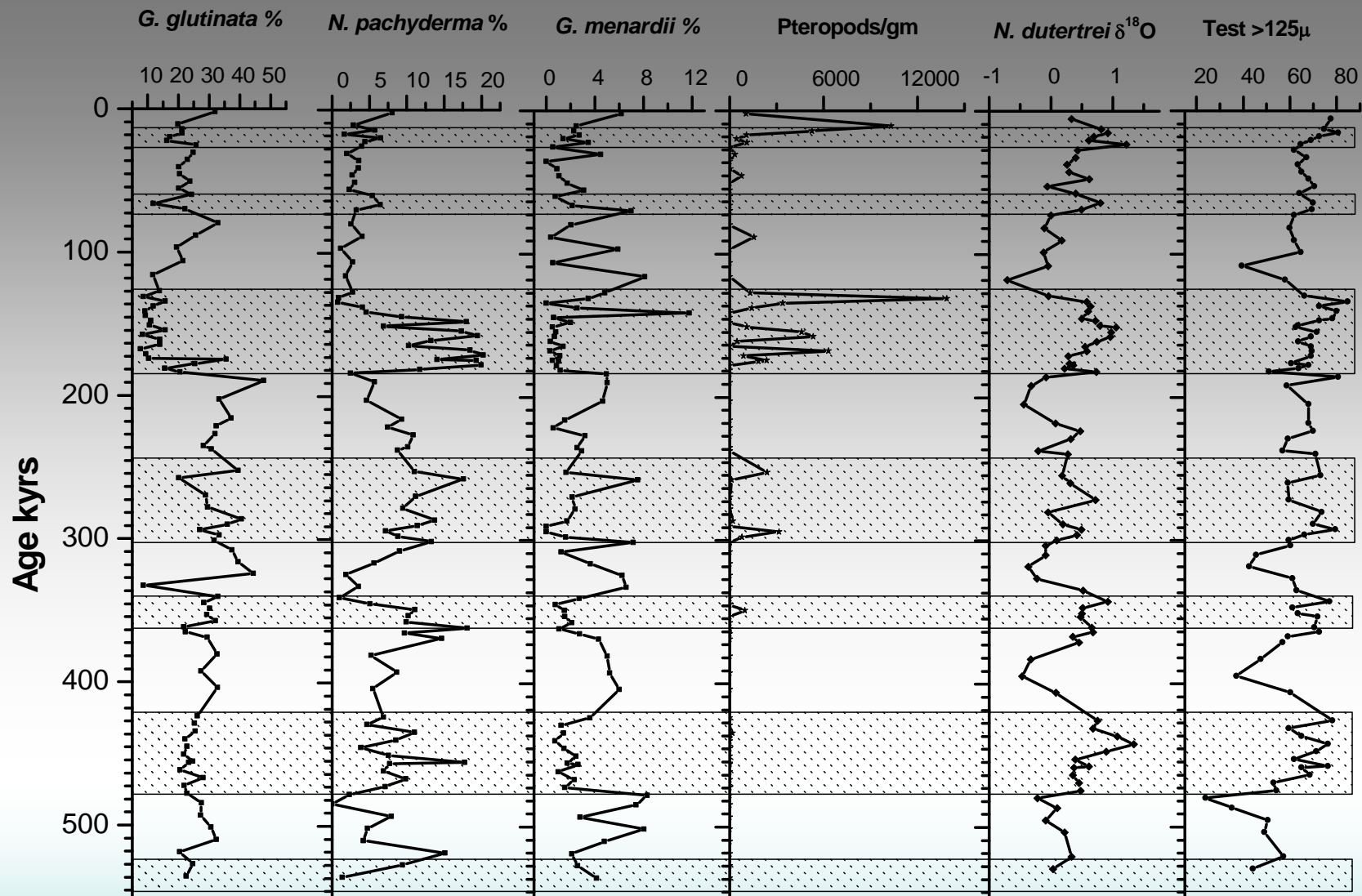
Globorotalia menardii
(dissolution resistant species)



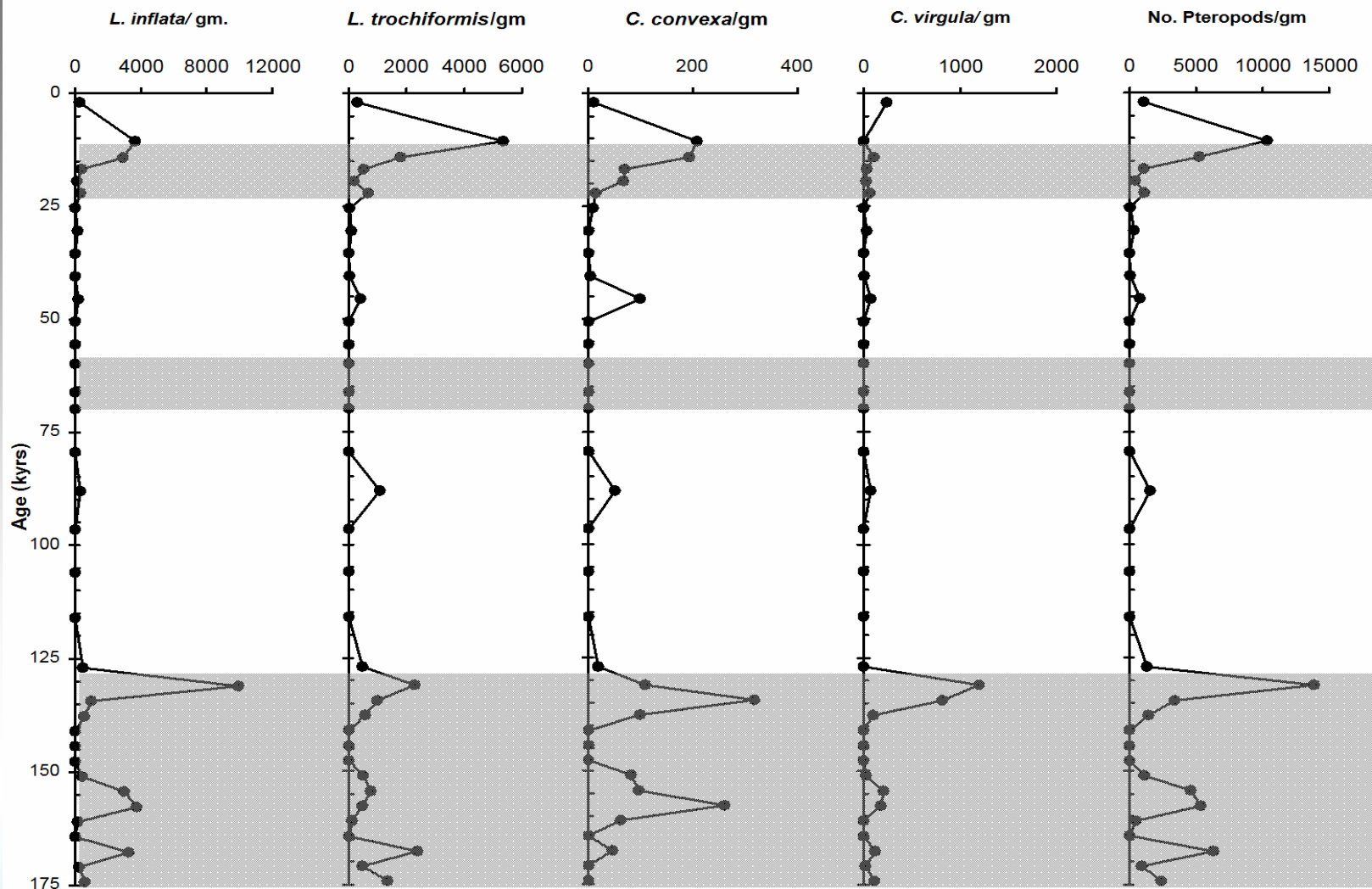
Globigerinoides ruber
(Non-upwelling, oligotrophic species)



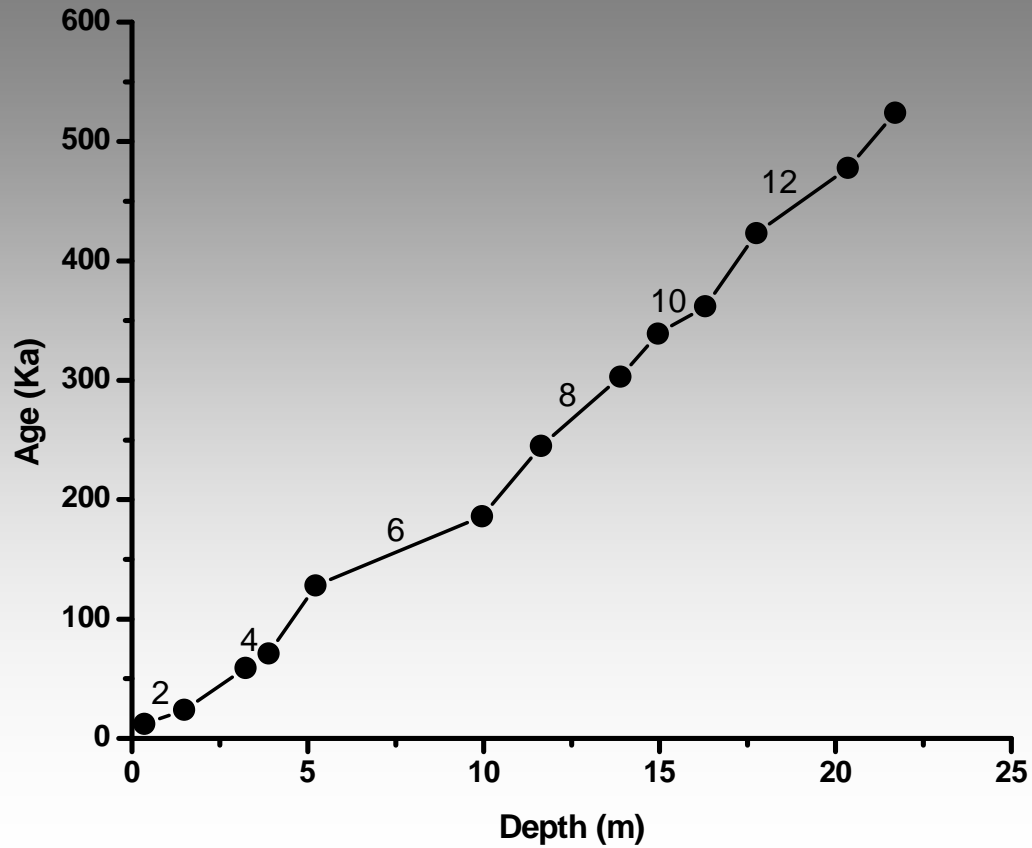
Time series plots of relative abundance of *Globigerinina glutinata*, *Neogloboquadrina pachyderma*, *Neogloboquadrina dutertrei*, *Globorotalia menardii*, *Globigerina bulloides* and *Globigerinoides ruber* at ODP Site 728A (Horizontal bars with dots represent glacial stages).



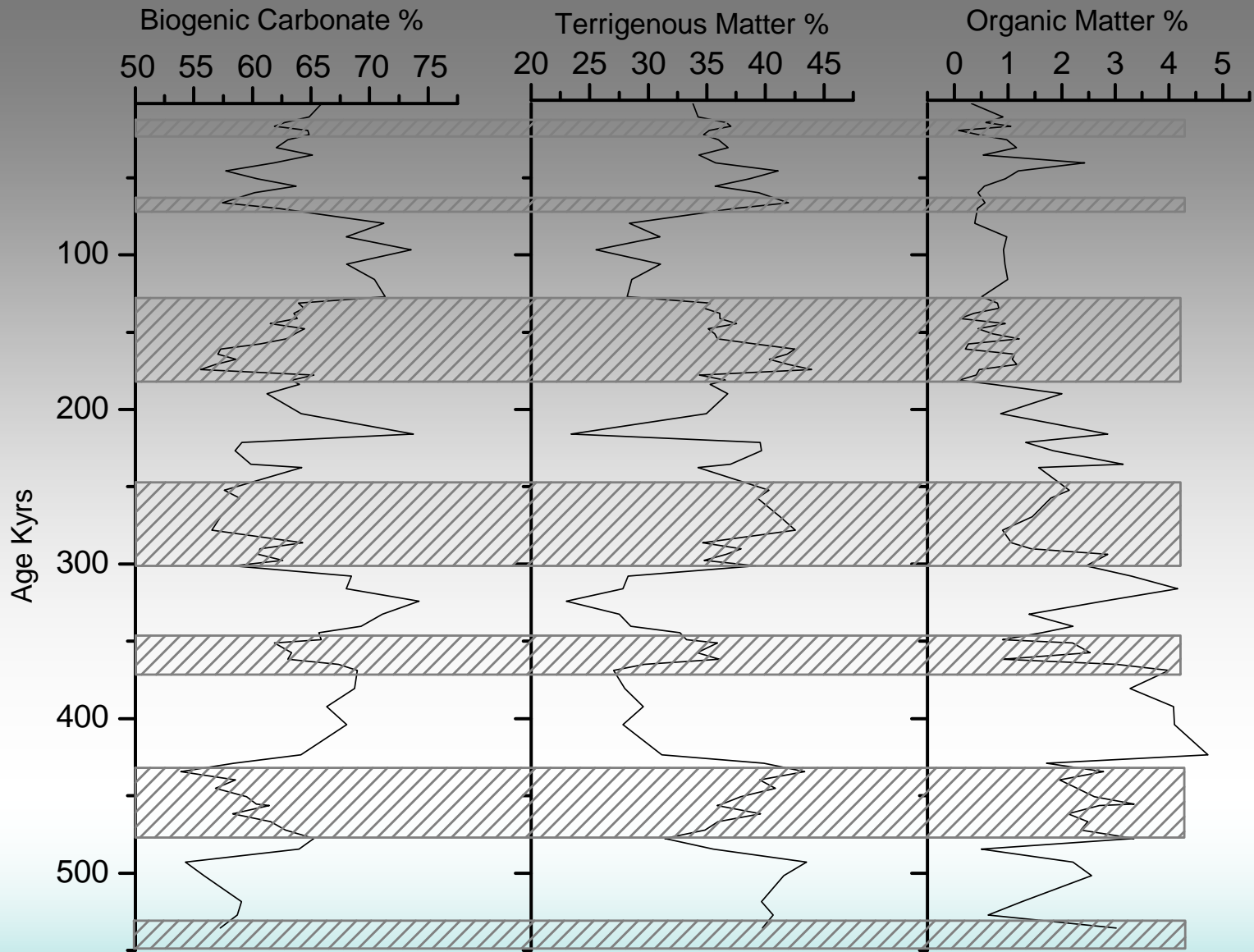
Time series plots of relative abundances of *G. glutinata*, *N. pachyderma* and *G. menardii*; number of pteropods/gm; planktic foraminiferal $\delta^{18}\text{O}$ values and foraminiferal fragmentation (Steens et al., 1991) at ODP Site 728A (Horizontal bars with dots represent glacial stages).



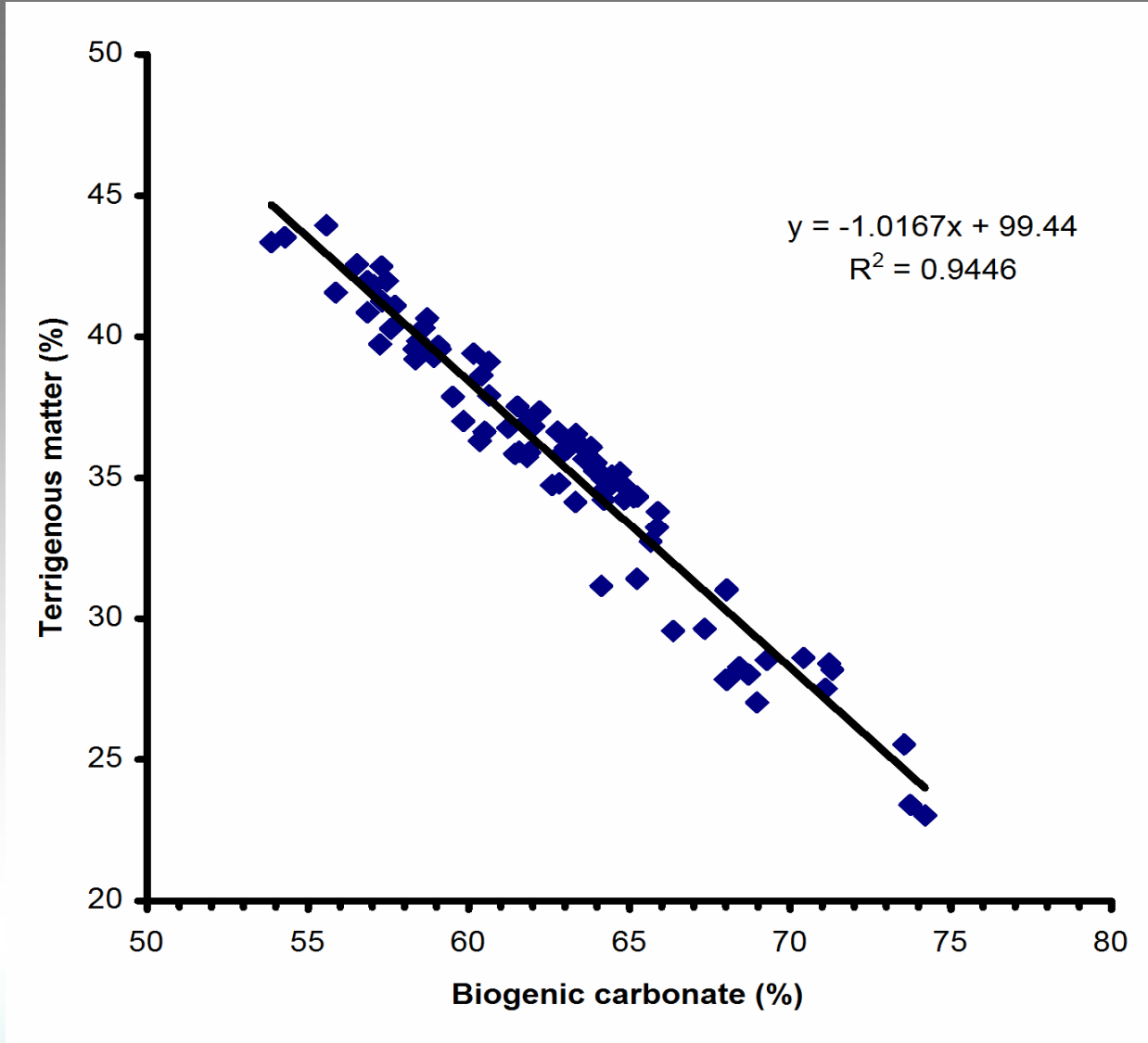
Downcore variations in numerical abundance (no. of specimens/gm dry sediment) of selected Pteropod species, Total no. of Pteropod shells/gm dry sediment. (Rai et al., 2008)



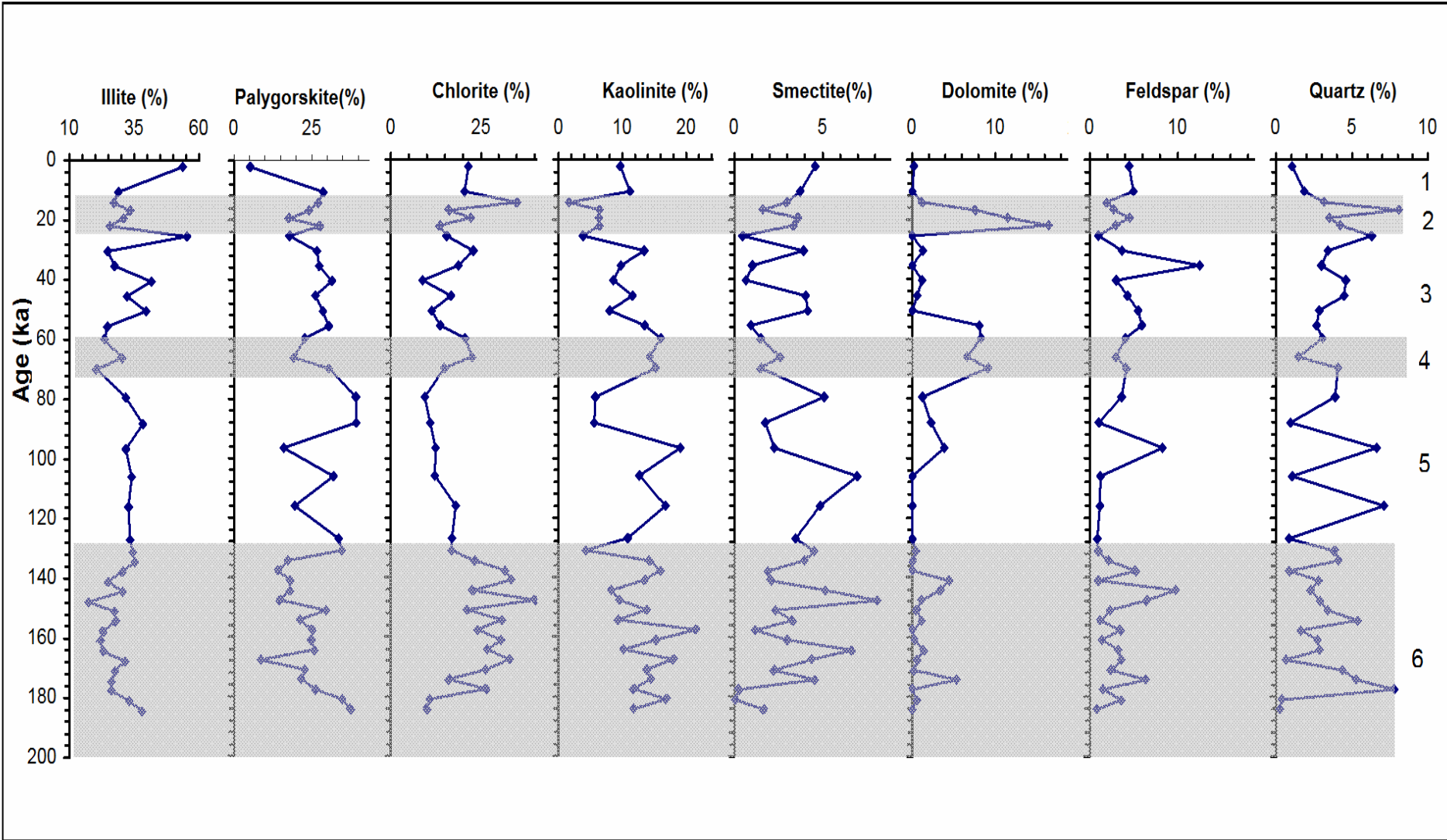
Sediment accumulation rates (Even numbers on the curve indicate intervals of glacial stages).



Time series plots of biogenic carbonate (%), terrigenous matter (%) and organic matter (%) at ODP Site 728A (Horizontal bars with dots represent glacial stages).



Scatter plot between biogenic carbonate (wt%) and terrigenous matter (wt%) showing inverse relation.



Down core variations in relative abundances of clay and non-clay minerals at ODP Site 728A (Das et al., 2008). Shaded area represents glacial stages. Nos 1-6 indicate MIS.

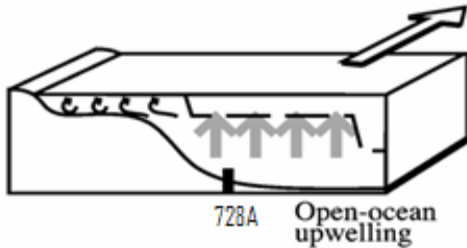
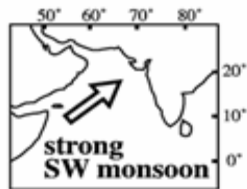
Chlorite : Northeast monsoon wind during glacial intervals.

Kaolinite : Southwest monsoon winds during interglacial intervals.

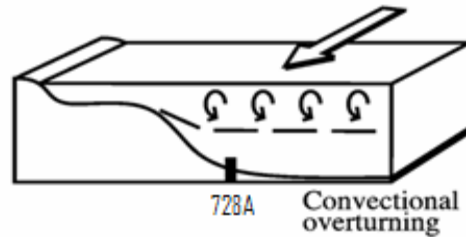
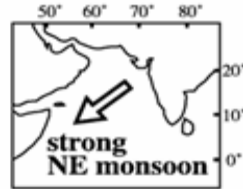
<Northern Hemisphere summer perihelion & winter aphelion>



(a) Type 1 July insolation high during interglacial period

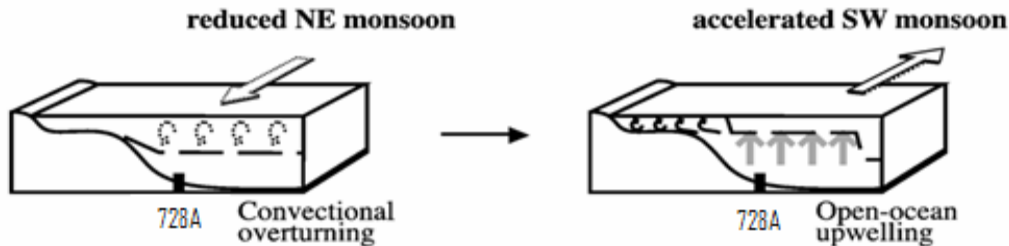


(b) Type 2 January insolation low during glacial period



<Glacial to interglacial transition periods of MIS 6/5.5 and 2/1>

(c) Type 3



Schematic illustration of different scenarios describing the changing surface water conditions driven by insolation changes during (a) interglacial periods, (b) glacial periods, and (c) transitions from glacial to interglacial periods. A rough dashed line indicates changes in the mixed layer depth. (after Ishikawa and Oda, 2007)

Paleoceanographic Inferences

1. Strong SW summer monsoon was mainly responsible for the intense surface productivity due to coastal & open ocean upwelling during interglacial intervals .
2. Less upwelling during glacial intervals due to weaker SW summer monsoon.
3. Strong NE winter monsoon during glacial periods resulted into more effective surface water convection.
4. Transitional intervals from glacial to interglacial show extreme intensification of SW monsoon & reduced NE winter monsoon resulting into intense open ocean upwelling and surface productivity.
5. Higher organic matter influx in the water column during interglacial times enhanced the intensity of OMZ and dissolution.

Thus, the upwelling, surface productivity, OMZ and dissolution in the NW Arabian Sea are alternately influenced by both SW and NE monsoon during interglacial and glacial intervals respectively.

Thank You